

AD-A043 517

ARMY ELECTRONICS COMMAND FORT MONMOUTH N J  
PHOTOVOLTAGE CHARACTERIZATION OF MOS CAPACITORS. (U)  
AUG 77 R L STREEVER, J J WINTER, F ROTHWART  
ECOM-4515

F/G 9/1

UNCLASSIFIED

NL

1 OF 1  
AD  
A043517



END  
DATE  
FILMED  
9 -77  
DDC



12 2

7 Research and Development Technical Report

1 ECOM-4515

AD A 043517

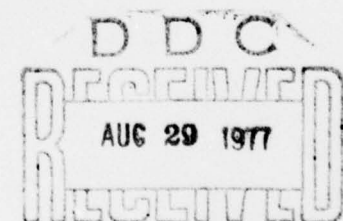
# PHOTOVOLTAGE CHARACTERIZATION OF MOS CAPACITORS

R. L. Streever  
J. J. Winter  
F. Rothwarf

Electronics Technology & Devices Laboratory

August 1977

DISTRIBUTION STATEMENT  
Approved for public release;  
distribution unlimited.



9 A

AD No.

DDC FILE COPY

ECOM

US ARMY ELECTRONICS COMMAND FORT MONMOUTH, NEW JERSEY 07703

## **NOTICES**

### **Disclaimers**

The findings in this report are not to be construed as an official Department of the Army position, unless so designated by other authorized documents.

The citation of trade names and names of manufacturers in this report is not to be construed as official Government indorsement or approval of commercial products or services referenced herein.

### **Disposition**

Destroy this report when it is no longer needed. Do not return it to the originator.

UNCLASSIFIED

SECURITY CLASSIFICATION OF THIS PAGE (When Data Entered)

REPORT DOCUMENTATION PAGE		READ INSTRUCTIONS BEFORE COMPLETING FORM
1. REPORT NUMBER 14 <b>ECOM-4515</b>	2. GOVT ACCESSION NO.	3. RECIPIENT'S CATALOG NUMBER
4. TITLE (and Subtitle) 6 <b>PHOTOVOLTAGE CHARACTERIZATION OF MOS CAPACITORS,</b>	5. TYPE OF REPORT & PERIOD COVERED	
7. AUTHOR(s) 10 <b>R.L./Streever, J.J./Winter F./Rothwarf</b>	6. PERFORMING ORG. REPORT NUMBER	
8. PERFORMING ORGANIZATION NAME AND ADDRESS <b>Electronic Materials Research Technical Area US Army Electronics Technology &amp; Devices Lab Fort Monmouth, NJ DRSEL-TL-ES</b>	9. CONTRACT OR GRANT NUMBER(s)	
10. CONTROLLING OFFICE NAME AND ADDRESS <b>US Army Electronics Command DRSEL-TL-ES Fort Monmouth, NJ 07703</b>	11. PROGRAM ELEMENT, PROJECT, TASK AREA & WORK UNIT NUMBERS 16 <b>61102A</b> <b>1L161102AH47/S7 051</b>	
12. MONITORING AGENCY NAME & ADDRESS (if different from Controlling Office) 9 <b>Research and development technical rept.</b>	13. REPORT DATE 11 <b>August 1977</b>	
14. DISTRIBUTION STATEMENT (of this Report) <b>Approved for public release; distribution unlimited.</b>	15. NUMBER OF PAGES <b>11</b>	
15. DISTRIBUTION STATEMENT (of the abstract entered in Block 20, if different from Report)	16. SECURITY CLASS. (of this report) <b>UNCLASSIFIED</b>	
16. SUPPLEMENTARY NOTES <b>This paper was presented at the Third International Symposium on Silicon Materials Science &amp; Technology, Philadelphia, PA, May 8-13, 1977, and published in the Proceedings of the Third International Symposium on Silicon Materials Science &amp; Technology, "Semiconductor Silicon 1977," May 1977.</b>	17. DECLASSIFICATION/DOWNGRADING SCHEDULE	
17. KEY WORDS (Continue on reverse side if necessary and identify by block number) <b>Photovoltage Metal-oxide-semiconductor capacitors Surface states</b>	18. DISTRIBUTION STATEMENT (of this Report) <b>12 14 p.</b>	
18. ABSTRACT (Continue on reverse side if necessary and identify by block number) <b>Surface photovoltage, capacitance and conductance measurements have been made on various metal-oxide-semiconductor (MOS) capacitors fabricated on p-type Si wafers. Curves of photovoltage plotted against dc sample bias are found to exhibit structure arising from surface state effects which correlates well with that observed in the C-V/G-V curves. In the region near the middle of the Si bandgap the surface state density can be reduced by about an order of magnitude by annealing. An equivalent circuit approach is used to relate the photovoltage to the electrical parameters</b>		

DD FORM 1 JAN 73 1473

EDITION OF 1 NOV 65 IS OBSOLETE

UNCLASSIFIED

SECURITY CLASSIFICATION OF THIS PAGE (When Data Entered)

037620

1B

## CONTENTS

ACCESSION FOR	
NTIS	White Section <input checked="" type="checkbox"/>
DOC	Buff Section <input type="checkbox"/>
UNANNOUNCED <input type="checkbox"/>	
JUSTIFICATION	
BY	
DISTRIBUTION/AVAILABILITY CODES	
DDC	AVAIL. DOC/OF SPECIAL
A	

	<u>Page</u>
I INTRODUCTION	1
II THEORETICAL MODEL	2
III EXPERIMENTAL	3
A. Photovoltage System	3
B. Preliminary Experiments	4
C. Photolithographic Samples	4
IV DISCUSSION	4
A. Capacitance Data	4
B. Conductance Data	6
C. Photovoltage Data	6
V CONCLUSION	7
ACKNOWLEDGEMENT	7
VI REFERENCES	7

## FIGURES

1. Equivalent circuit of a p-type MOS device	9
2. Real component of photovoltage at different frequencies	9
3. C-V and G-V curves for annealed sample	10
4. C-V and G-V curves for unannealed sample	10
5. Real component of photovoltage at 200 Hz for annealed and unannealed photoresist samples	11
6. Plot of $C_S/C_{OX}$ for annealed and unannealed photoresist samples	11



## PHOTOVOLTAGE CHARACTERIZATION OF MOS CAPACITORS

R.L. Streever, J.J. Winter and F. Rothwarf  
US Army Electronics Technology & Devices Laboratory (ECOM)  
Fort Monmouth, New Jersey 07703

### ABSTRACT

Surface photovoltage, capacitance and conductance measurements have been made on various metal-oxide-semiconductor (MOS) capacitors fabricated on p-type Si wafers. Curves of photovoltage plotted against dc sample bias are found to exhibit structure arising from surface state effects which correlates well with that observed in the C-V/G-V curves. In the region near the middle of the Si bandgap the surface state density can be reduced by about an order of magnitude by annealing. An equivalent circuit approach is used to relate the photovoltage to the electrical parameters.

### I Introduction

Studies of the surface photovoltage, which is the change in surface potential accompanying the creation by light of excess carriers in a semiconductor, have been extensively reported in the literature.<sup>1</sup> The possibility of using scanning photovoltage methods to evaluate the interfaces of large scale integrated (LSI) metal-oxide-semiconductor (MOS) devices has created renewed interest in such studies.<sup>2</sup> Preliminary experiments in this direction were made on MOS capacitors to see if one could correlate scanning photovoltages with conventional C-V/G-V measurements.

For evaluation purposes an array of MOS capacitors is usually formed by depositing Al contact dots on oxidized Si wafers either with mechanical masks or by photolithographic techniques. If the Al contacts are made sufficiently thin ( $\sim 150$  Å), so that they are essentially transparent to visible light, photovoltage studies can be performed on the individual capacitors. In the present investigation, we have carried out such studies by using as the light source a He-Ne (632.8 nm) laser which could be focused to a spot size of about one micron on the sample surface.

From the point of view of wafer evaluation two types of photovoltage studies are possible. First, one can scan the focused laser beam over a given contact and use the photovoltage variations as a means of detecting microstructure.<sup>2</sup> Second, by chopping the laser beam, one can measure the dc component of the photovoltage at a fixed point on a given contact. Thus, one can try to detect slow systematic variations in the photovoltage at different points on the contact or from contact

to contact. It is this latter approach that was used in the present investigation.

To correlate the photovoltage measurements directly with C-V measurements, we have carried out a theoretical and experimental investigation of the variation of photovoltage with dc bias and its relation to the C-V curves. We show that the photovoltage versus bias ( $V_p$ -V) curves can give similar information to that obtained with conventional admittance (G-V/C-V) measurements. The photovoltage measurements have the added advantage that small regions of the surface can be probed for uniformity of properties.

## II Theoretical Model

To analyze the dependence of photovoltage on sample bias or surface potential we use an equivalent circuit approach. This has an advantage over more conventional approaches<sup>1</sup> in that it gives expressions for the photovoltage explicitly as a function of frequency and directly in terms of the capacitances and conductances associated with the equivalent circuit of the MOS capacitor.

A simplified equivalent circuit for a p-type MOS capacitor is shown in Fig. 1. This is essentially the same circuit used by Saks<sup>3</sup> to discuss conductance measurements and by Nakhmanson<sup>4</sup> to discuss the photovoltage. Except for the addition of  $G_o$  and  $C_o$ , the circuit represents a simplification of the equivalent circuit described by Lehovc and Slobodskoy.<sup>5</sup>  $G_o$  and  $C_o$  represent the recombination conductance and capacitance.  $G_p$  and  $G_n$  are the surface state conductances for majority and minority carriers, respectively.  $C_I$ ,  $C_D$  and  $C_s$  are the inversion layer, depletion layer and surface state capacitance, respectively, while  $C_{ox}$  is the insulator capacitance. If the semiconductor is strongly doped so that the carrier concentration ratio  $n_o/p_o$  is small (for a p-type material) then to this approximation one can represent the effect of the chopped light source by an ac current source  $I_L$  in parallel with  $G_o$ .<sup>4</sup>

The circuit of Fig. 1 can be used to give an expression for  $V_p$ , the photovoltage developed between the Si surface (point S of Fig. 1) and the bulk substrate. The general expression is rather complex, however, and it is of interest to consider limiting cases.

### Case I

No surface states  $C_s=G_p=G_n=0$  and  $C_o$  small  $\omega C_o \ll G_o$ . Then  $V_p$  is given simply by

$$V_p = -\frac{|I_L|}{G_o} \left( \frac{C_I}{C_I + C_D} \right) \left[ 1 + j\omega \left( \frac{C_I C_D}{C_I + C_D} \right) \frac{1}{G_o} \right]^{-1} \quad (1)$$

In the low frequency limit the imaginary component of  $V_p$  (the component out of phase with respect to  $I_L$ ) vanishes. The real component will increase from zero as the semiconductor is biased into inversion and will approach a limiting value of  $I_L/G_o$  in the strong inversion limit.

### Case II

#### Low frequency limit

In the low frequency limit the following expression for the real component of  $V_p$  can be obtained

$$\text{Real } V_p = -\frac{|I_L|}{G_o} \frac{1}{(C_D + C_I + C_S)} \left\{ \frac{C_I + C_s \left( \frac{G_n}{G_n + G_p} \right)}{1 + \left( \frac{G_n G_p}{G_n + G_p} \right) \frac{1}{G_o}} \right\} \quad (2)$$

We see that in general there is both a surface state and an inversion layer contribution to  $V_p$ .

The surface states also make a contribution to the out-of-phase part of  $V_p$ . The expression is rather complex, and since it won't be needed in an experimental analysis we omit it here.

### III Experimental

#### A. Photovoltage System

The photovoltage-bias experiments were carried out using a scanning photovoltage system similar to that described by DiStefano and Viggiano.<sup>6</sup> The system uses a He-Ne 632.8 nm (visible red) laser which is focused on the sample to a spot size of about one micron. When the system is operated in the normal scanning mode, an ac photovoltage signal is induced as the light spot is scanned across a defect. In the present study a light chopper was added to the system so that an ac signal could be developed independently of the scanning. In the typical experiment the light spot was focused near the center of a given contact and a plot of photovoltage versus sample bias was obtained. It was determined that the  $V_p$ -V curves were essentially the



same from spot to spot for a given contact so that meaningful comparisons to C-V/G-V measurements, which average over a whole contact, could be made. On a given sample, results for different contacts were also quite similar. The photovoltage was measured by monitoring the ac current through  $C_{ox}$  with a sensitive current amplifier. In such a detection scheme the measured current is  $90^\circ$  out of phase with respect to the photovoltage. A lock-in amplifier was used to enable real and imaginary components of  $V_p$  to be measured separately.

#### B. Preliminary Experiments

Preliminary studies were done using MOS capacitors fabricated on  $\langle 100 \rangle$  orientation p-type Si wafers with resistivities of 2-4  $\Omega\text{-cm}$ . The wafers were thermally oxidized in dry  $O_2$  at  $1000^\circ\text{C}$  to a thickness of 870  $\text{\AA}$ . An array of transparent Al front contact dots approximately 150  $\text{\AA}$  thick were deposited by electron beam evaporation through a mechanical mask. Thicker contacts were deposited on the edge of the transparent ones to facilitate electrical connection and an Al back contact was also deposited.

Curves showing the real component of  $V_p$  versus sample bias taken at different frequencies of the chopped laser source are shown in Fig. 2. The photovoltage variations about zero bias are due to the presence of surface states and occur in the region around weak inversion.

#### C. Photolithographic Samples

In order to increase the surface state effects a second set of MOS capacitors were fabricated on  $\langle 111 \rangle$  orientation p-type Si wafers with resistivities of 1.5 to 2.0  $\Omega\text{-cm}$ . The dry thermal oxide was about 1,000  $\text{\AA}$  thick. Transparent Al contacts (approximately 125  $\text{\AA}$  thick and 2 mm square) were defined by photoresist techniques and deposited by electron beam evaporation. Smaller area thicker contacts (approximately 10,000  $\text{\AA}$  thick) were also deposited to facilitate electrical connection. One set of samples was left unannealed and one set (from the same wafer) was given a final  $N_2$  anneal at  $500^\circ\text{C}$ .

Capacitance and conductance measurements made with a PAR C-V plotter on representative contacts of the annealed and unannealed samples are shown in Figs. 3 and 4, respectively. Photovoltage-bias curves showing the real component of  $V_p$  at 200 Hz for the two types of samples are given in Fig. 5.

### IV Discussion

#### A. Capacitance Data

The capacitance curves of Fig. 4 indicate a large distribution

of surface states in the unannealed sample and also a large fixed positive charge distribution which displaces the curves along the voltage axis. Both the surface states and the fixed charge are reduced by annealing, the voltage displacement being about one volt smaller in the annealed sample.

The variation of the surface state capacitance  $C_s$  with sample bias can be obtained from the low frequency capacitance data. At low frequencies the C-V curves approach the quasistatic ones and the measured parallel capacitance  $C_m$  is given simply by<sup>7</sup>

$$\frac{C_m}{C_{ox}} = \frac{C_D + C_I + C_s}{C_D + C_I + C_s + C_{ox}} \quad (3)$$

Letting  $C_T$  be the low frequency capacitance that would be measured in the absence of surface states (i.e., the value of  $C_m$  when  $C_s=0$ ), we then have

$$\frac{C_s}{C_{ox}} = \frac{(C_m/C_T - 1)}{(1 - C_m/C_{ox})(C_{ox}/C_T - 1)} \quad (4)$$

In accumulation and depletion where  $C_I=0$ , the high frequency capacitance curves coincide with the low frequency ones when  $C_s=0$ . Consequently, in this range  $C_T$  can be obtained from the high frequency capacitance curves. In inversion  $C_T$  can be obtained from standard calculated C-V curves.

Values of  $C_s/C_{ox}$  calculated from Eq. (4) are shown in Fig. 6 for annealed and unannealed samples. In the unannealed sample  $C_s$  is seen to peak right around midgap (about -3 volts for this sample) where the slower surface states are most effective. By contrast the annealed sample shows surface state peaks to either side of midgap (about -2 volts for this sample). This is consistent with the shoulders observed in the C-V curves for the annealed sample. The shoulders on the inversion side of midgap tend to be obscured by the inversion capacitance.

The surface states may be due to the electron beam irradiation to which the samples were subjected during evaporation of the contacts. In the photoresist process the Al layer for the thick contacts was deposited over the whole surface and then selectively etched away. Consequently, the whole surface received a large irradiation. The large density of surface states near midgap in irradiated samples would be consistent with the findings of Ma.<sup>8</sup>

## B. Conductance Data

From the conductance data of Figs. 3 and 4 we see that conductance peaks occur in both depletion and inversion suggesting that we must consider both majority and minority carrier response. As has been discussed by Saks,<sup>5</sup> surface state conduction can occur in two separate channels. For a p-type device these can be the majority carrier path through  $G_p$  or the minority carrier path through  $G_n$  and  $G_o$  (refer to Fig. 1). If  $G_o$  is much greater than  $G_p$  and  $G_n$  at midgap then both minority as well as majority carrier response has to be considered on a nearly equal basis.

The part of the measured parallel conductance due to surface states can be written<sup>9</sup>

$$\frac{G_m}{\omega} = \frac{C_s \omega \tau C_{ox}^2}{(C_{ox} + C_D + C_s)^2 + \omega^2 \tau^2 (C_{ox} + C_D)^2} \quad (5)$$

Here  $\tau$  is the surface state time constant. For a given frequency this expression peaks at two values of surface potential. One in depletion when  $\omega \tau_p = (C_{ox} + C_D + C_s) / (C_{ox} + C_D)$  and one in inversion when  $\tau_n$  replaces  $\tau_p$ . At high frequencies the peaks occur where  $\tau$  is small (near the bandgap edges). At lower frequencies the peaks come together and merge near midgap where  $\tau_p$  and  $\tau_n$  become comparable. This is just the behavior observed experimentally.

Values of  $C_s$  obtained using Eq. (5) were found to agree well with those obtained from C-V data and are shown in Fig. 6.

## C. Photovoltage Data

We turn now to an analysis of the photovoltage data taken at 200 Hz. In the annealed sample we see a surface state shoulder at about -2.7 volts and a peak at about -1 volt occurring respectively in depletion and inversion (as noted previously midgap in this sample occurs at about -2 volts). These peaks correlate well with surface state peaks in the conductance data and with those observed in the  $C_s$  plot. The unannealed sample shows a broad surface state response from about -1.0 volt to about -6 volts which also agrees well with the low frequency conductance peak or with the peak in the  $C_s$  plot at about -3 volts (around midgap).

Although the photovoltage correlates well with  $C_s$ , there does appear to be a discrepancy with the theory of Section II. According to Eq. (2) the surface state photovoltage should be small in depletion when  $G_n / (G_n + G_p) \ll 1$ . According to the experimental result, however, surface state response occurs in both depletion and inversion (on both

sides of midgap). It seems likely therefore that the equivalent circuit of Fig. 1 (which in the original Lehovec-Slobodskoy<sup>5</sup> version assumed a negligible recombination rate in the space charge layer) is not the correct one to use.

For the case of infinite recombination rate in the space charge layer Lehovec and Slobodskoy<sup>5</sup> describe a different circuit which puts  $G_p$  and  $G_n$  in parallel. Such a circuit would give surface state response in both depletion as well as in inversion. Provided  $C_s$  was symmetric about midgap, the surface state photovoltage would be symmetric also. It seems that such a circuit could explain, therefore, the photovoltage as well as the conductance data and such a model will be discussed more fully in a future paper.

#### V. Conclusion

The surface state distribution has been evaluated for p-type MOS samples using admittance and photovoltage techniques and the results correlate well with each other. As might be expected, we find the surface state distribution to vary markedly with annealing. At midgap the surface states are about an order of magnitude smaller in the annealed sample.

These studies should be helpful in the analysis of scanning photovoltage displays. They also point to the possibility of using scanning photovoltage methods for quantitative diagnostic studies of LSI structures.

#### Acknowledgement

The authors gratefully acknowledge T.H. DiStefano for some initial discussions concerning the development of the scanning photovoltage system and the efforts of E. Ahlstrom, E. Kostyk, N. Korolkoff and J. Finnegan in preparing samples for us.

#### VI. References

1. For extensive references to surface photovoltage studies see the recent papers by N. Kasupke and M. Henzler, Surface Sci. 54, 111 (1976) and D.L. Lile, Surface Sci. 34, 337 (1973).
2. D.L. Lile and N.M. Davis, Solid-State Electron. 18, 699 (1975); J.W. Philbrick and T.H. DiStefano, in 13th Annual Proceedings, Reliability Physics (Las Vegas, Nevada, April 1975).
3. N.S. Saks, Solid-State Electron. 18, 737 (1975).



4. R.S. Nakhmanson, Sov. Phys. Semicond. 1, 687 (1967); *ibid.* 4, 372 (1967); R.S. Nakhmanson, Solid State Electron. 18, 617 (1975).
5. K. Lehovec and A. Slobodskoy, Solid-State Electron. 7, 59 (1964).
6. T.H. DiStefano and J.M. Viggiano, IBM J. Res. Dev. 18, 94 (1974).
7. A. Goetzberger, E. Klausmann and M.J. Schulz, CRC Critical Reviews in Solid State Science 6, 1 (1976)
8. T.P. Ma, Appl. Phys. Lett. 27, 615 (1975).
9. S.M. Sze, Physics of Semiconductor Devices, Wiley-Interscience, New York (1969) p. 447.

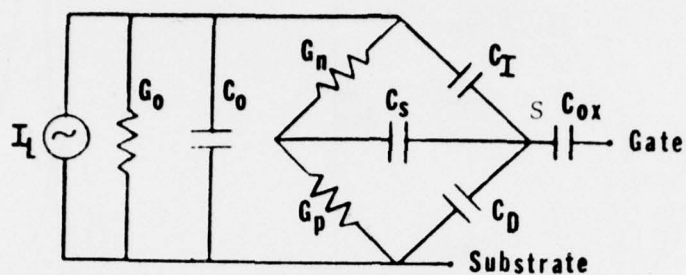


Fig. 1. Equivalent circuit of a p-type MOS device.

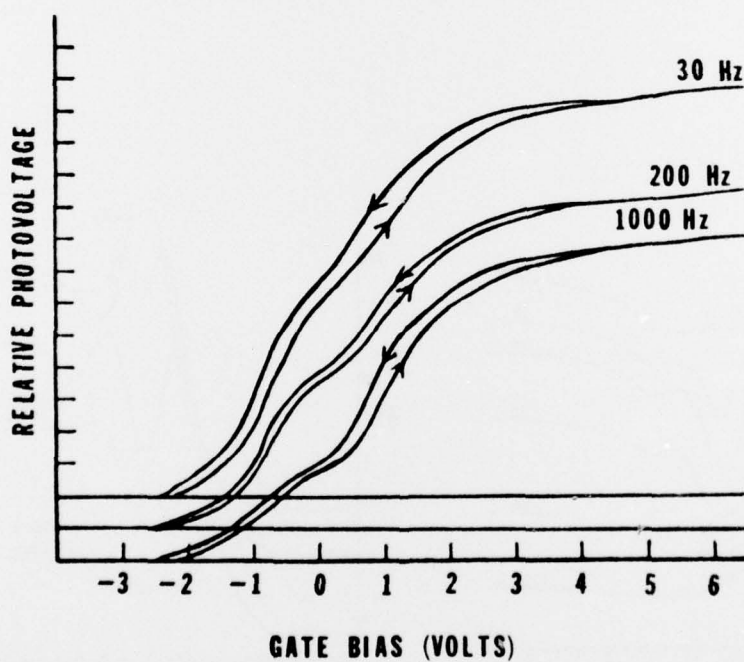


Fig. 2. Real component of photovoltage at different frequencies.

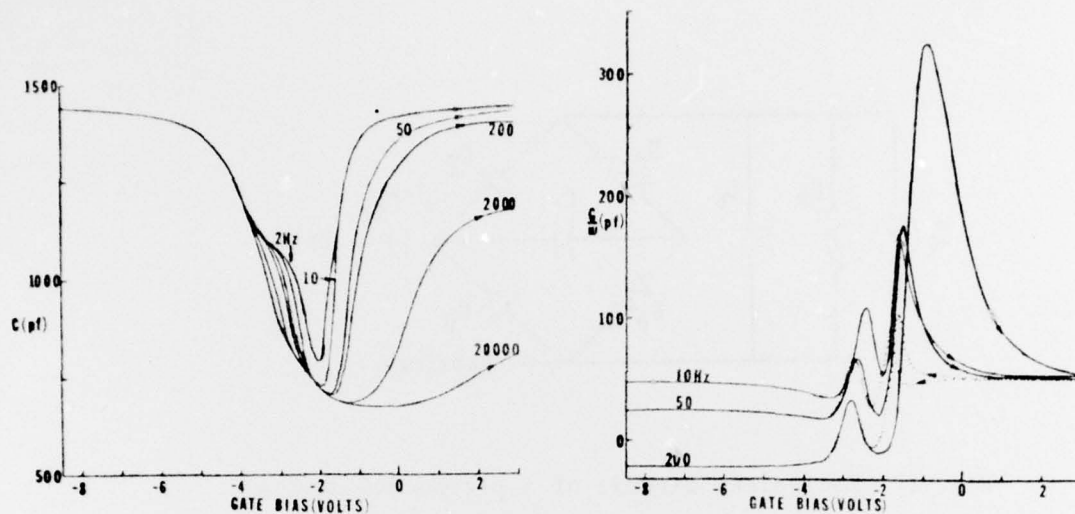


Fig. 3. C-V and G-V curves for annealed sample.

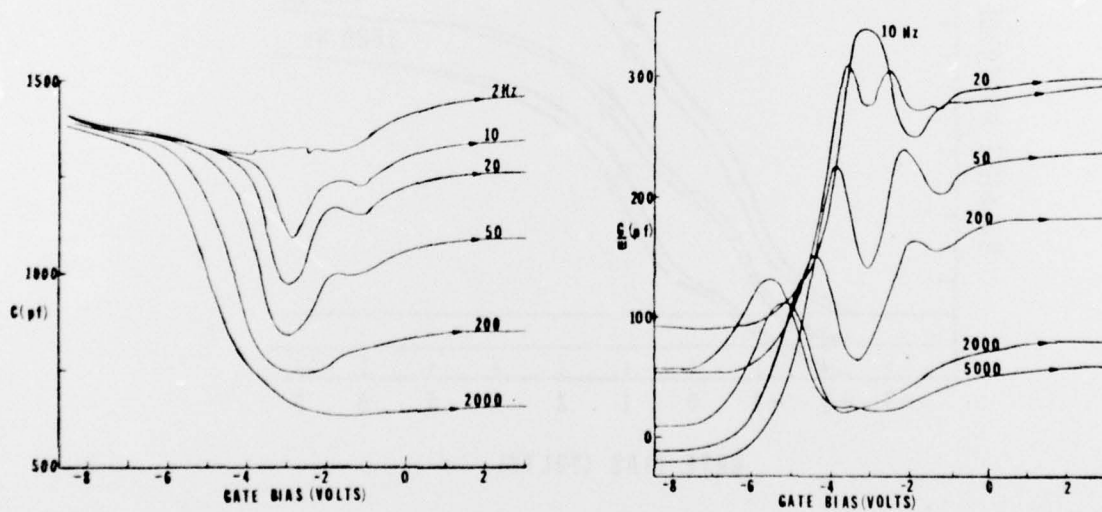


Fig. 4. C-V and G-V curves for unannealed sample.

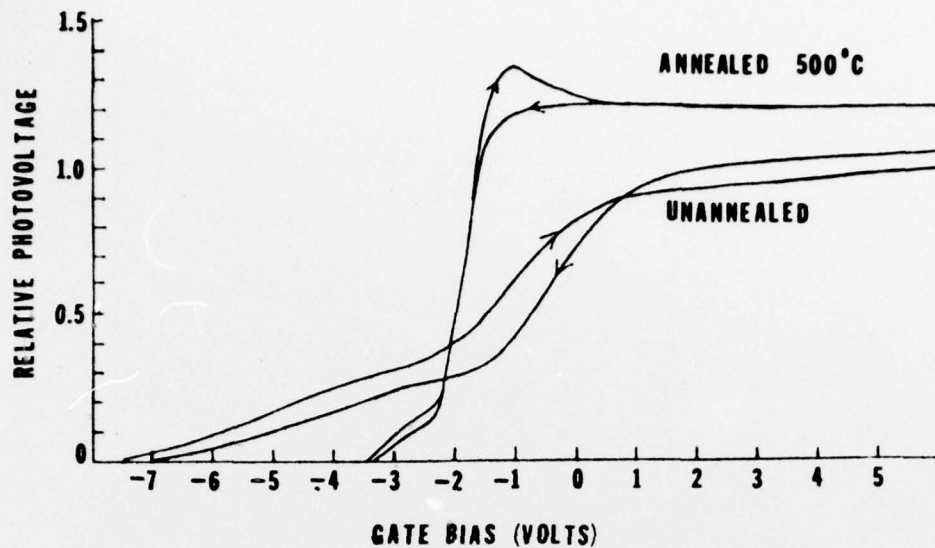


Fig. 5. Real component of photovoltage at 200 Hz for annealed and unannealed photoresist samples.

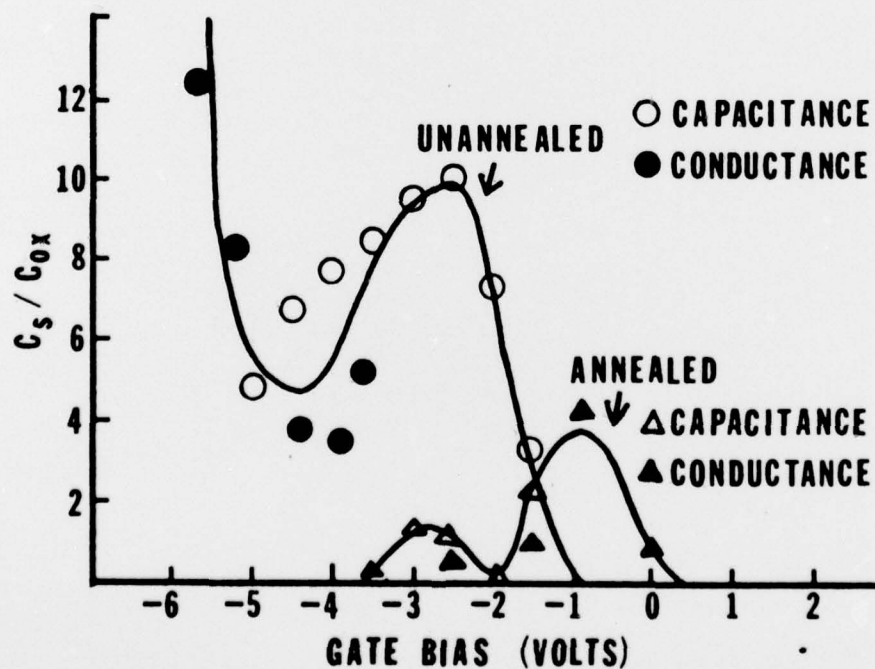


Fig. 6. Plot of  $C_s/C_{ox}$  for annealed and unannealed photoresist samples.